

## The Growth and Congregation of Minor Phase in Immiscible Cu-Fe Alloys

Jun Ting ZHANG<sup>1</sup>, You Hong WANG<sup>2</sup>, Xiao Chao CUI<sup>1\*</sup>, Jin Bao LIN<sup>1</sup>

<sup>1</sup> School of Applied Science, Taiyuan University of Science and Technology, Taiyuan 030024, China

<sup>2</sup> Institute of Materials Science and Technology, Taiyuan University of Science and Technology, Taiyuan 030024, China

crossref <http://dx.doi.org/10.5755/j01.ms.19.4.3568>

Received 20 February 2013; accepted 12 May 2013

The growth and congregation of minor phase in immiscible Cu-Fe alloys were investigated. Results showed that the Brown motion was strongly affected by the initial number of the separated droplets. With the increase of initial numbers of droplets, the time needed for completing the Brown congregation reduced. The calculation confirmed that increasing the radiuses of droplets would lead to the decrease of the time for congregation completed. As the increases of the undercooling and the droplet radius, the ratio of Stokes motion velocity to Marangoni motion velocity increased.

**Keywords:** phase separation; congregation; undercooling; Cu-Fe alloy.

### 1. INTRODUCTION

For some Cu-based alloys, such as Cu-Co, Cu-Fe, Cu-Cr and Cu-Nb etc., a metastable liquid phase separation occurs when the liquid metal is undercooled into the metastable miscibility gap [1]. In recent years, great attention has been paid to the investigation of these immiscible alloys. Many techniques, such as the electromagnetic levitation [2, 3], drop tube processing [4], fluxing purification technique [5, 6] and gas atomization [7, 8], were employed to investigate the factors (such as the composition, the cooling rate and the undercooling) that influence the solidification structure.

However, much work on the Cu-based alloys was focused on the investigation of the microstructure morphology [1–8] and the evaluation of the stable and metastable phase diagram [9–12]. Many aspects for these alloys, such as the process of the phase separation in undercooled melts, nucleation, growth and solidification of separation phase, were not completely understood. In recently years, Cu-Fe alloy has been one of the most interested fields in material science for their high-strength and high-conductivity properties. In this work, in order to better understand the growth process of the separated spheres, Cu75Fe25 alloy was produced by melt-fluxing, then, the growth and congregation of minor phase in immiscible Cu75Fe25 alloy were investigated in detail.

### 2. EXPERIMENTAL PROCEDURES

High-purity (99.99 %) copper and iron were used to prepare the Cu75Fe25 alloy by melt-fluxing in combination with cyclic superheating technique. The melts were first heated to the desired temperature using high frequency induction heating facility, and then the superheating-cooling procedure was repeated several times. To investigate the influence of the undercooling on the solidification structure in immiscible Cu-Fe alloys, the different undercooling was obtained by the cyclic superheating method. When the maximum heating

temperature was about 1600 K, the obtained maximum undercooling was 115 K.

The thermal history of the sample was monitored by a standard PtRh30-/PtRh6 thermocouple and a temperature recorder with 1 ms response time. According to standard metallographic procedures, the samples were cross sectioned, processed and etched. The microstructures of as-prepared samples were analyzed by using HITACHI S-4800 field emission scanning electron microscopy.

### 3. RESULTS AND DISCUSSIONS

The microstructural images of the as-prepared Cu75Fe25 alloy at different undercooling are shown in Fig. 1. Only Fe-rich dendrites could be observed in Fig. 1, a, it indicated that the solidification of Cu75Fe25 alloy was in the way of normal solidification at  $\Delta T = 35$  K. When the undercooling ( $\Delta T$ ) increased to 45 K, there were two types of microstructures morphologies: dendrites and spheres, as shown in Fig. 1, b. Because the Fe-rich spherical particle was the typical structure of liquid separation, it could be deduced that metastable liquid separation occurred in Cu75Fe25 alloy.

When the undercooling of melt exceeds a critical value, the undercooled liquid (L) separates into the Fe-rich liquid ( $L_1$ ) and the Cu-rich liquid ( $L_2$ ) [13]. In order to diminish the interface energy in the Cu75Fe25 melt, the spherical particles were formed and free in the Cu-rich matrix. For a given composition, the relative amounts of  $L_1$  and  $L_2$  were expected to follow the ‘lever rule’. And the amount of  $L_1$  liquid increased with the increase of the undercooling [2]. Just as presented in Fig. 1, b, c and d, when the undercooling of the Cu75Fe25 melt increased to 45 K, 70 K and 115 K, the area fraction of the Fe-rich spheres in the entire region of microstructures was 5 %, 30 % and 45 %, respectively, and the amount of the Fe-rich dendrites in the Cu-rich matrix reduced corresponding. In particular, such a phenomenon that some spheres adhered together each other could be seen from Fig. 1, c and d. Furthermore, some fine Fe-rich droplets, which failed to coagulate and grow up before the solidification, stayed in the periphery of a large particle. It could be inferred from

\*Corresponding author. Tel.: +86-0351-6998165; fax.: +86-0351-6998165. E-mail address: wangsimai1225@163.com (X. C. Cui)

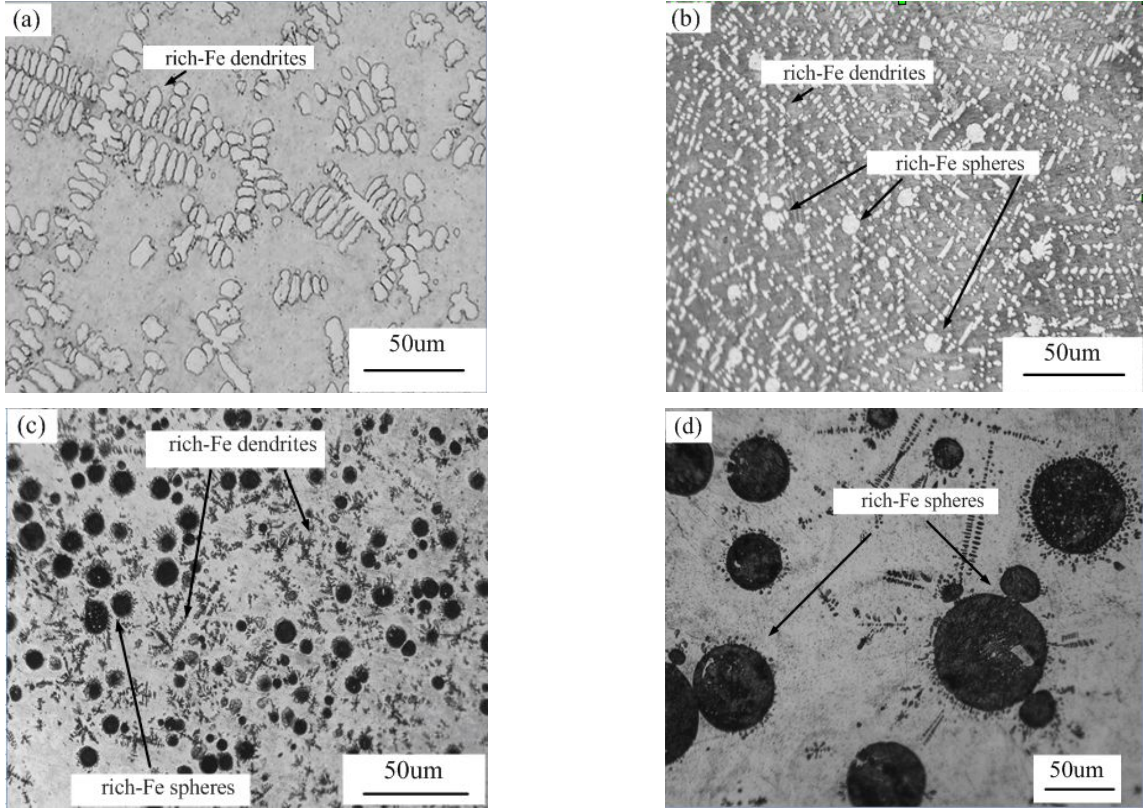


**Fig. 1.** The microstructures of as-solidified Cu75Fe25 alloy at different undercooling: a –  $\Delta T = 35$  K; b –  $\Delta T = 45$  K; c –  $\Delta T = 70$  K; d –  $\Delta T = 115$  K

this that the collision with each other and congregation should be undergo by the separated droplets before solidification.

According to the dynamical theory of phase separation, the growth and congregation of the separated minor phase were mainly caused by Brown congregation, Stokes and Marangoni congregation [14]. The number change of droplets ( $N(t)/N_0$ ) caused by Brown congregation can be calculated by the formula [15] below:

$$\frac{N(t)}{N_0} = \frac{9\eta_m^2}{(3\eta_m + 2N_0 \cdot K_B \cdot T \cdot t)^2}, \quad (1)$$

where  $K_B$  is Boltzmann constant,  $\eta_m$  is viscosity of matrix,  $T$  is temperature of the melt.

On the assumption initial numbers ( $10^{20}$ ,  $10^{15}$ , and  $10^{10}$ , respectively) of droplets, the number change of droplets ( $N(t)/N_0$ ) by Brown motion was calculated utilizing the above formula (1) and is shown in Fig. 2. It indicates that the time needed for completing the Brown congregation reduced with the increase of the initial number of droplets. When the initial numbers were  $10^{20}$  and  $10^{10}$ , the numbers of droplets decreased by 90 % in 1 s and  $10^3$  s, respectively. It signified that the number change of droplets was affected drastically by the initial number of droplets by Brown motion. As a result of Brown motion, the number of droplets reduced while the size of droplets enlarged.

According to Smoluchowski's collision formula [16], a function of droplet number dependence on time can be obtained:

$$N(t) = \frac{N_0}{1 + W_0 \cdot N_0 \cdot t/2}, \quad (2)$$

where  $W_0$  and  $N_0$  is initial collision volume and droplet number at  $t = 0$  s, respectively. For two droplets with radiuses as  $r_d$  and  $r_{d1}$ , Stokes collision volume ( $W_s$ ) and Marangoni collision volume ( $W_m$ ) can be described as follows [17]:

$$W_s(r_d, r_{d1}) = \pi(r_d + r_{d1})^2 |V_s(r_d) - V_s(r_{d1})|; \quad (3)$$

$$W_m(r_d, r_{d1}) = \pi(r_d + r_{d1}) |V_m(r_d) - V_m(r_{d1})|, \quad (4)$$

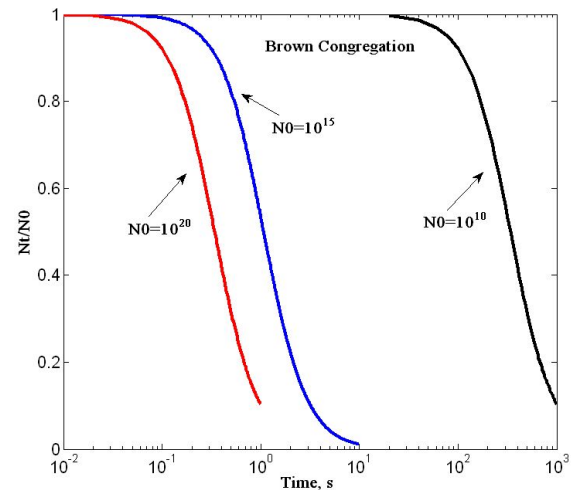


**Fig. 2.** The number change of droplets as a function of time under Brown motion

The Stokes motion velocity can be expressed as [18]:

$$V_s \approx \frac{2}{3} \frac{(\rho_m - \rho_d) \left( \frac{\eta_d}{\eta_m} + 1 \right) g}{(3\eta_d + 2\eta_m)} (r_d)^2, \quad (5)$$

where  $(\rho_m - \rho_d)$  represents the density difference of Fe-rich droplets and Cu-rich matrix,  $\eta_d$  and  $\eta_m$  is the viscosity of Fe-rich phase and Cu-rich phase, respectively,  $g$  is the gravitational acceleration, and  $r_d$  is the average radius of the liquid droplets.

The Marangoni motion velocity of the liquid droplet  $V_m$  is given by [19]:

$$V_m \approx \frac{-2r_d}{3\eta_d + \eta_m} \cdot \frac{\lambda_m}{\lambda_d + 2\lambda_m} \cdot \frac{\partial \rho}{\partial T} \cdot \frac{\partial T}{\partial x}, \quad (6)$$

where  $\rho$  is the interfacial tension between the droplet and matrix,  $\lambda_m$  and  $\lambda_d$  are the thermal conductivity of the liquid droplet and matrix liquid phases, respectively,  $T$  is the absolute temperature and  $\chi$  is the distance corresponding to the change of  $T$ .

The number change of the droplets by Stokes motion and Marangoni migration was calculated utilizing the formula (2) combination with the formula (5) and (6), respectively. The Fig. 3 given the relationship curves between the number change of droplets and time under Stokes motion and Marangoni migration. Under the radiuses as  $r_{d1} = 10 \mu\text{m}$ ,  $r_d = 20 \mu\text{m}$  and  $r_{d1} = 5 \mu\text{m}$ ,  $r_d = 10 \mu\text{m}$ , the time needed for completing the Stokes congregation was approximately 0.1 s and 1 s, respectively; while the numbers of droplets by Marangoni migration decreased by 80 % in 0.1 s and 1 s, respectively. Therefore, it could be concluded that the time needed for completing the Stokes congregation and Marangoni migration reduced with increasing the radius of droplets, respectively, and the Stokes motion could play a more important role on congregation of liquid droplets than Marangoni motion.

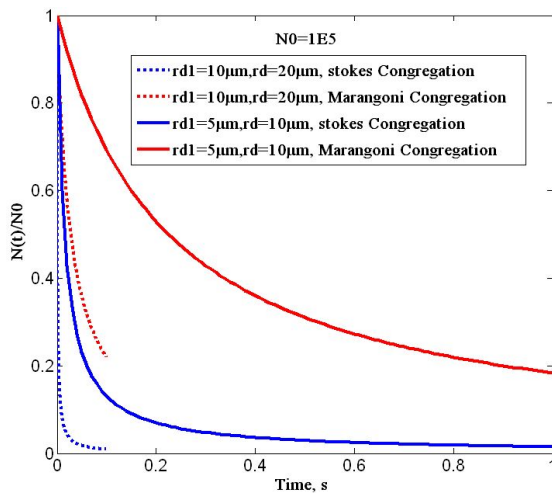


**Fig. 3.** The relationship curves between the number change of droplets and time under Stokes motion and Marangoni migration

Figure 4 demonstrated that the ratio of Stokes motion velocity to Marangoni motion velocity ( $V_s/V_m$ ) depends on the droplet radius and the undercooling of the melt. With undercooling of  $\Delta T = 115 \text{ K}$ , the value of  $V_s/V_m$  was 0.4585, 45.8517, and 183.4069, when the droplet radius  $r_d = 1 \mu\text{m}$ ,  $10 \mu\text{m}$  and  $20 \mu\text{m}$ , respectively. When undercooling  $\Delta T$  was 45 K, 70 K and 115 K, the value of  $V_s/V_m$  was 11.4629, 9.0611, and 2.8034, respectively, for a droplet with a radius of  $5 \mu\text{m}$ . These calculations meant

that the ratio  $V_s/V_m$  increased with the undercooling and droplet radius increasing. High undercooling and large droplets were available to improve the effect of Stokes motion.

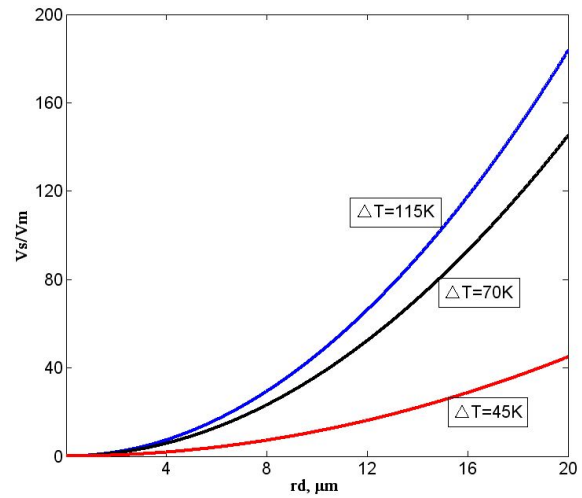


**Fig. 4.** The ratio of Stokes motion velocity to Marangoni motion velocity versus droplet radius

#### 4. CONCLUSIONS

The typical spherical structures were observed in the microstructure, when the undercooling of the Cu75Fe25 melt reached 45 K. The spherical particles were Fe-riched phase and generated from the metastable liquid separation.

Due to the Brown motion, the collision and amalgamation of the droplets were strongly influenced by the initial number of separated droplets in undercooled melt. The time needed for completing congregation reduced with the initial number of droplets increasing. The effects of Stokes motion and Marangoni migration on congregation of separated droplets were enhanced as the droplets radiuses enlarged. The calculation confirmed that the larger the radiuses of droplets were, the shorter the time for congregation completed was. Moreover, the ratio  $V_s/V_m$  increased with the increase of undercooling and droplet radius.

#### Acknowledgments

The authors are grateful to the financial support of the National Natural Science Foundation of China (No:51204117), the Natural Science Foundation for Young Scientists of Shanxi Province 2012021018-2 and Shanxi Scholarship Council of China (2011-079).

#### REFERENCES

1. **Chen, Y.-Z., Liu, F., Yang, G.-C., Xu, X.-Q., Zhou, Y.-H.** Rapid Solidification of Bulk Undercooled Hypoperitectic Fe-Cu Alloy *Journal of Alloys and Compounds* 427 (1-2) 2007: pp. L1-L5.
2. **Munitz, A., Abbaschian, R.** Microstructure of Cu-Co Alloys Solidified at Various Supercoolings *Metallurgical and Materials Transactions A* 27 (12) 1996: pp. 4049-4059.
3. **Munitz, A., Elder, S.-P., Abbaschian, R.,** Supercooling Effects in Cu-10 Wt Pct Co Alloys Solidified at Different

- Cooling Rates *Metallurgical Transactions A* 23 (6) 1992: pp. 1817–1827.
4. **Munitz, A., Abbaschian, R.** Two-melt Separation in Supercooled Cu-Co alloys solidifying in a Drop-tube *Journal of Materials Science* 26 (23) 1991: pp. 6458–6466.
  5. **Liu, N.** Investigation on the Phase Separation in Undercooled Cu-Fe Melts *Journal of Non-Crystalline Solids* 358 2012: pp. 196–199.  
<http://dx.doi.org/10.1016/j.jnoncrysol.2011.09.009>
  6. **Liu, N., Yang, G.-C., Yang, W., Liu, F., Yang, C.-L., Zhou, Y.-H.** Microstructure Evolution of Undercooled Fe-Co-Cu Alloys *Physica B* 406 (4) 2011: pp. 957–962.
  7. **He, J., Zhao, J.-Z.** Behavior of Fe-rich Phase during Rapid Solidification of Cu-Fe Hypoperitectic Alloy *Materials Science and Engineering A* 404 (1–2) 2005: pp. 85–90.
  8. **He, J., Zhao, J.-Z., Ratke, L.** Solidification Microstructure and Dynamics of Metastable Phase Transformation in Undercooled Liquid Cu-Fe Alloys *Acta Materialia* 54 (7) 2006: pp. 1749–1757.  
<http://dx.doi.org/10.1016/j.actamat.2005.12.023>
  9. **Kim, D.-I., Abbaschian, R.** The Metastable Liquid Miscibility Gap in Cu-Co-Fe Alloys *Journal of Phase Equilibria* 21 (1) 2000: pp. 25–31.  
<http://dx.doi.org/10.1361/105497100770340381>
  10. **Palumbo, M., Curiotto, S., Battezzati, L.** Thermodynamic Analysis of the Stable and Metastable Co-Cu and Co-Cu-Fe Phase Diagrams *Calphad* 30 (2) 2006: pp. 171–178.
  11. **Bamberger, M., Munitz, A., Kaufmsn, L., Abbaschian, R.** Evaluation of the Stable and Metastable Cu-Co-Fe Phase Diagrams *Calphad* 26 (3) 2002: pp. 375–384.
  12. **Banda, W., Georgalli, G.-A., Lang, C., Eksteen, J.-J.** Liquidus Temperature Determination of the Fe-Co-Cu System in the Fe-rich Corner by Thermal Analysis *Journal of Alloys and Compounds* 461 (1–2) 2008: pp. 178–182.
  13. **Curiotto, S., Pryds, N.-H., Johnson, E., Battezzati, L.** Effect of Cooling Rate on the Solidification of  $\text{Cu}_{58}\text{Co}_{42}$  *Materials Science and Engineering A* 449–451 2007: pp. 644–648.
  14. **Ratke, L., Diefenbach, S.** Liquid Immiscible Alloys *Materials Science and Engineering R: Reports* 15 (7–8) 1995: pp. 263–347.
  15. **Liu, N., Liu, F., Yang, W., Chen, Z., Yang, G.-C.** Movement of Minor Phase in Undercooled Immiscible Fe-Co-Cu Alloys *Journal of Alloys and Compounds* 551 2013: pp. 323–326.  
<http://dx.doi.org/10.1016/j.jallcom.2012.10.050>
  16. **Smoluchowski, M.-V.** Drei Vortrage uber Diffusion, Brownsche Bewegung und Koagulation von Kolloidteilchen *Zeitschrift fur Physik* 17 1916: pp. 557–585.
  17. **Jia, J., Zhao, J., Guo, J., Liu, Y.** Immiscible Alloys and Their Preparation Techniques. Harbin Institute of Technology, 2002.
  18. **Dai, F.-P., Cao, C.-D., Wei, B.-B.** Phase Separation and Rapid Solidification of Liquid  $\text{Cu}_{60}\text{Fe}_{30}\text{Co}_{10}$  Ternary Peritectic Alloy *Science in China Series G: Physics, Mechanics and Astronomy* 50 (4) 2007: pp. 509–518.
  19. **Ma, B.-Q., Li, J.-Q., Peng, Z.-J., Zhang, G.-C.** Structural Morphologies of Cu-Sn-Bi Immiscible Alloys with Varied Compositions *Journal of Alloys and Compounds* 535 2012: pp. 95–101.